THE JOURNAL OF PHYSICAL CHEMISTRY A

Article

Cite This: J. Phys. Chem. A XXXX, XXX, XXX−XXX

pubs.acs.org/JPCA

Photodissociation Dynamics of Ortho-Substituted Thiophenols at 243 nm

Jean Sun Lim, Hyun Sik You,[†] Songhee Han,[‡] and Sang Kyu Kim*

Department of Chemistry, KAIST, Daejeon 34141, Republic of Korea

Supporting Information

ABSTRACT: The photoinduced S−H (D) bond fission dynamics of four ortho-substituted thiophenols, 2-fluoro, 2-chloro, 2-bromo, and 2-methoxythiophenol at a pump wavelength of 243 nm, have been investigated by velocity-map imaging and high-level electronic structure calculations. The D atom images of the deuterated ortho-substituted thiophenols show much reduced $\tilde{X}/\tilde{A}$ branching ratios of the cofragment radicals over that of bare thiophenol. The angular distributions of the D fragment display negative anisotropies, indicating that transition dipole moments are perpendicular to the fast dissociating S−D bond axis. Initial excitation at 243 nm occurs directly to the $^1\pi\sigma^*$ state or to the $2^1\pi\pi^*$ state followed by efficient coupling to the $^1\pi\sigma^*$ state. The calculated potential energy curves for the $^1\pi\sigma^*$ or $2^1\pi\pi^*$ excited states of the ortho-substituted thiophenols along the CCS−D torsion angle (ϕ) display minima at the nonplanar structures, whereas all of the states for bare thiophenol present minima at the planar geometries. This different topology of the ortho-substituted thiophenols in the excited states induces the wide spread of the reactive flux along the ϕ coordinate on the repulsive surface as it should experience significant torque with respect to ϕ during the fragmentation. This encourages the dissociating molecules to follow the adiabatic path at the conical intersection between the ground and the $^1\pi\sigma^*$ states at extended S−D bond lengths, giving rise to decreased $\tilde{X}/\tilde{A}$ branching ratios, demonstrating that the excited-state molecular structure dictates the nonadiabatic transition probability.

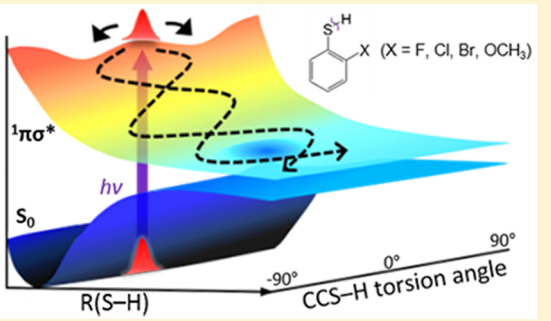

1. INTRODUCTION

A multitude of studies on the photoinduced H(D) atom elimination reaction of aromatic enols and azoles have been reported, since the theoretical works of Sobolewski and Domcke provided a new paradigm for $^1\pi\sigma^*$-mediated nonradiative decay.[1−4] The S−H bond dissociation of thiophenol belongs to the family of the $^1\pi\sigma^*$-mediated photochemistry[5−14] and was first studied at 243 nm in the gas phase over a decade ago.[15] The first singlet excited state is a bound $1^1\pi\pi^*$ (S_1) state, while the next excited state is a $^1\pi\sigma^*$ (S_2) state repulsive along the S−H bond elongation coordinate. The $^1\pi\sigma^*$ state intersects with the $1^1\pi\pi^*$ and ground (S_0) states, generating the conical intersections (CIs) of CI-1 and CI-2, respectively. The product branching is determined at CI-2, at which $^1\pi\sigma^*$ and S_0 diabatically correlate to the ground ($\tilde{X}^2B_1$) and excited ($\tilde{A}^2B_2$) states of the thiophenoxyl radical, respectively. In this photodissociation reaction, the $C_6H_5S\cdot$ ($\tilde{X}$) + H channel is produced only nonadiabatically by funneling through CI-2, whereas $C_6H_5S\cdot(\tilde{A})$ + H is yielded on the adiabatic pathway by avoiding the CI-2. Due to an appropriate energy difference between the two product channels, the experimental detection of the fragment by, for example, the velocity-map imaging (VMI) technique[16] could be used to measure the $\tilde{X}/\tilde{A}$ product branching ratio. Investigations on thiophenol have been extensive, covering a wide range of photoexcitation wavelength,[17−19] substituted derivatives,[20−24] time-resolved experiment,[25] and theoretical calculations.[26−30] The CCSH torsional angle (ϕ) was identified as the most important coordinate in determining the product branching, as theoretical studies have shown that the torsion mode is the strongest coupling mode in both CIs,[26] and the shapes of potential energy curves (PECs) along the ϕ coordinate are quite critical in explaining the experimental results.[20,21] The para substitution to the thiophenol influences the shape of the PECs along the ϕ coordinate in the S_0 state, whereas the excited electronic states are negligibly affected, having the same minima at ϕ = 0°,[20,21] and this makes it possible to manipulate the nonadiabatic transition probability at CI-2 by the conformational changes in the S_0 state. For the ortho-substituted thiophenols, the resonant two-photon ionization (R2PI) spectra for the S_1-S_0 transitions were reported for 2-fluorothiophenol (2-FTP) and 2-chlorothiophenol (2-CTP).[12] It is interesting to note that no R2PI signal was observed for thiophenol due to its ultrashort S_1 lifetime, indicating an increased S_1 state lifetime under ortho substitution.[22]

In this work, we studied the 243 nm photodissociation dynamics of 2-FTP, 2-CTP, 2-bromothiophenol (2-BTP), and

Received: January 26, 2019
Revised: March 9, 2019
Published: March 11, 2019

DOI: 10.1021/acs.jpca.9b00803
J. Phys. Chem. A XXXX, XXX, XXX−XXX

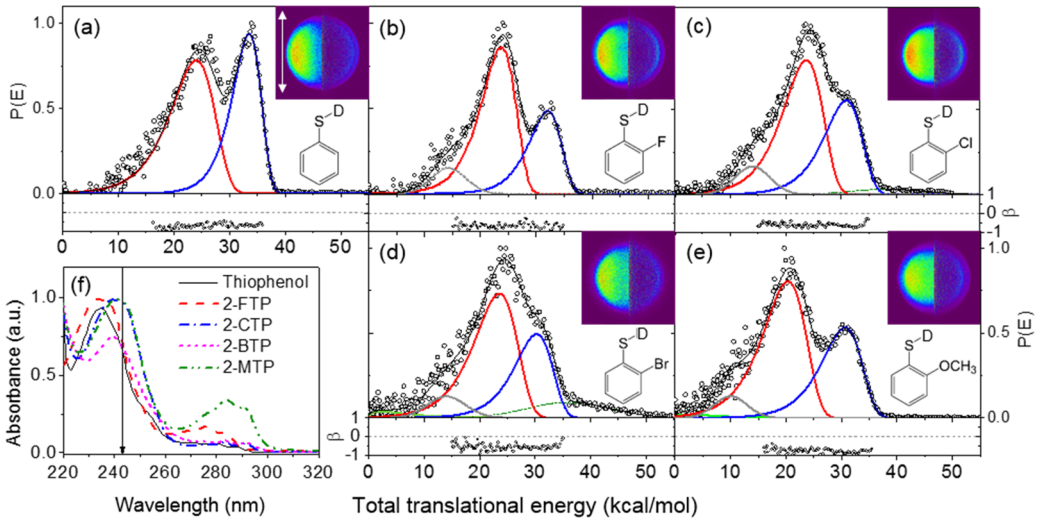

Figure 1. Total translational energy distributions and anisotropy parameters (black circles) of (a) thiophenol-d_1, (b) 2-fluorothiophenol-d_1 (2-FTP-d_1), (c) 2-chlorothiophenol-d_1 (2-CTP-d_1), (d) 2-bromothiophenol-d_1 (2-BTP-d_1), and (e) 2-methoxythiophenol-d_1 (2-MTP-d_1) obtained at 243 nm. Two Gumbel functions in red and blue solid lines correspond to the $\tilde{A}$ and $\tilde{X}$ states of the fragment radicals, respectively. Gaussian function in gray dashed line represents the contribution from the $1^1\pi\pi^*$ state, whereas the multiphoton background is depicted by the green dashed line. Raw (left half) and reconstructed (right half) D images are displayed in the inset. White arrows indicate the laser polarization direction. (f) UV absorption spectra of thiophenol (black line), 2-FTP (red dashed line), 2-CTP (blue dash−dotted line), 2-BTP (magenta short dashed line), and 2-MTP (olive dash-dot-dotted line) in hexanes at room temperature. Arrow indicates the position of 243 nm.

2-methoxythiophenol (2-MTP). These thiophenols adopt cis-planar structures in the ground states, and direct or indirect excitation to the $^1\pi\sigma^*$ state is expected at 243 nm. The halogen substitution, from F to I, was investigated on phenol,[31,32] revealing that the O−H fragmentation dynamics at short wavelength excitation (near 243 nm) is actually similar to that of bare phenol. Significant differences in energetics involved in photodissociation reactions of phenols and thiophenols hamper direct comparison though as far as the substitution effect on dynamics is concerned. Here, we found that ortho substitution of thiophenol gives rise to a substantial influence on the nonadiabatic transition probability at the conical intersection, demonstrating that the topology of the excited-state potential energy surface dictates the nonadiabatic dynamics.

2. EXPERIMENTAL SECTION

Thiophenol, 2-FTP, 2-CTP, 2-BTP, and 2-MTP were purchased from Tokyo Chemical Industry (TCI). The deuterated samples for the VMI experiment were obtained by mixing with D_2O; 2-MTP-d_1 was supplied by MediGen Inc. All of the samples were heated to 45−85 °C. The resulting vapors were carried out with 3 bar He gas, expanded through a nozzle orifice (General valve series 9; 0.5 mm diameter) into the vacuum chamber, and collimated with a skimmer (Beam dynamics, 1 mm diameter). The VMI of the D fragment was recorded using (2 + 1) ionization at an excitation wavelength 243.0 nm, which was obtained by frequency doubling of the dye laser output (Lumonics, HD-500) pumped by the third harmonic of a Nd:YAG laser (Continuum, Surelite II). The wavelength of the laser pulse was continuously scanned over the Doppler width of the D fragment, while the image was being recorded. The polarization direction of the pulse was parallel to the plane of the phosphor screen. The ions were velocity mapped onto a microchannel plate (MCP) coupled to a phosphor screen and recorded with a charge-coupled device (CCD) camera. The image was sent to a PC and processed using the IMACQ acquisition software.[33] The resulting 2D images were reconstructed to the 3D distribution using the BASEX algorithm.[34] The Jacobian factor was considered when converting the velocity distribution into the total translational energy distribution. The anisotropy parameter (β), which describes the angular distribution of photofragments, was obtained from the equation of $I(\theta) = \frac{\sigma}{4\pi}[1 + \beta \cdot P_2(\cos(\theta))]$, where θ is the angle of the fragment velocity vector with respect to the polarization vector of the pump laser, P_2 is the second-order Legendre polynomial, and σ is the absorption cross section. The images were energetically calibrated using the O image from O_2 at 225 nm.

Computational Details. To predict the most stable conformation, the S_0 geometries of the 2-BTP and 2-MTP molecules were optimized by the B3LYP[35] and second-order Mollet−Plesset perturbation theory (MP2)[36] methods. The $\tilde{A}$ and $\tilde{X}$ state radical energies were calculated by the B3LYP/aug-cc-pVTZ[37] and multiconfigurational second-order perturbation theory (CASPT2)(9,8)[38]/cc-pVTZ methods. The (9,8) active space comprises the three pairs of π/π^* orbitals and the n_π and n_σ orbitals of sulfur. The vertical excitation energies were calculated by the equation-of-motion coupled cluster single and doubles (EOM-CCSD)[39]/aug-cc-pVTZ and TD-HCTH[40]/6-311++G(3df,3pd) levels of theory. For the PECs along ϕ, the S_0 geometries were optimized using the MP2/aug-cc-pVTZ level of theory. The vertical excitation energies for the first three singlet excited states were obtained using the EOM-CCSD level of theory. The ϕ value was varied, while the other remaining nuclear coordinates were maintained at those of the S_0 MP2 geometries. The density functional theory (DFT) and MP2 calculations were performed using Gaussian 09,[41] while the torsional PECs were obtained using Molpro 2010.1.[42]

DOI: 10.1021/acs.jpca.9b00803
J. Phys. Chem. A XXXX, XXX, XXX−XXX

Table 1. $\tilde{X}/\tilde{A}$ Branching Ratios for the 243 nm Photodissociation of the S−D Bond and β Values of Thiophenol-d_1, 2-FTP-d_1, 2-CTP-d_1, 2-BTP-d_1, and 2-MTP-d_1

	thiophenol-d_1	2-FTP-d_1	2-CTP-d_1	2-BTP-d_1	2-MTP-d_1
$\tilde{X}/\tilde{A}$	0.78 ± 0.04	0.53 ± 0.02	0.66 ± 0.04	0.60 ± 0.02	0.62 ± 0.03
β^b	−0.73	−0.71	−0.63	−0.57	−0.76

[a]The error bar was determined from the fitting procedure (Supporting Information). [b]Weighted averages in the range of 15−35 kcal/mol.

3. RESULTS AND DISCUSSION

The experimental D images obtained at the 243 nm photoexcitation of thiophenol-d_1, 2-FTP-d_1, 2-CTP-d_1, 2-BTP-d_1, and 2-MTP-d_1 are displayed in the insets of Figure 1 together with the reconstructed images (right halves). Two rings are observed: the outer ring, which corresponds to the $\tilde{X}$ state of the fragment radical, is stronger than the inner ring, which corresponds to the $\tilde{A}$ state for thiophenol but rather weak for the rest of the molecules. The total translational energy distributions derived from these images (black circles in Figure 1) reveal that relative to that of bare thiophenol, the $\tilde{X}$ state yields for the ortho-substituted thiophenols are much reduced, indicating that the nonadiabatic transition probabilities are quite diminished by the ortho substitution. The red and blue solid lines in Figure 1 correspond to the $\tilde{A}$ and $\tilde{X}$ state fragment radicals, respectively (fitting procedure in the Supporting Information). The energy gaps between the $\tilde{A}$ and the $\tilde{X}$ states of the radical (Figure 1) from fits are roughly estimated to be 9.5, 8.3, 7.2, 6.7, and 10.3 kcal/mol for thiophenol-d_1, 2-FTP-d_1, 2-CTP-d_1, 2-BTP-d_1, and 2-MTP-d_1, respectively. Generally, these values follow the order of the calculated energy gaps (Table S1). The smallest gap for 2-BTP should be responsible for the indistinguishable rings in the D image. The S_0 structures of the ortho-substituted thiophenols here are all considered to adopt the cis-planar form in the supersonic jet (Table S2).[22] The angular distributions of all of the images are perpendicular to the polarization of the linearly polarized pump laser pulse, indicating that the transition dipole moments (TDMs) are perpendicular to the S−H(D) bond axis and the dissociation time scale is shorter than the rotational dephasing time. One may be tempted to assign the 243.0 nm transition as $(^1\pi\sigma^*)-S_0$ because the TDM direction of the $^1\pi\sigma^*$ states for the thiophenol systems is perpendicular to the ring plane. However, for all of the molecules of interest, the TDMs of the $2^1\pi\pi^*$ states, according to the EOM-CCSD and TD-DFT calculations, are also predicted to have angles, even though those are in plane, closer to the direction that is perpendicular to the S−H(D) bond axis (Tables S3 and S4 for 2-BTP and 2-MTP, respectively).[18,19,22] Therefore, the negative anisotropy parameters observed in the range from −0.6 to −0.8 indicate that an initial excitation occurs to the $^1\pi\sigma^*$ and/or $2^1\pi\pi^*$ states. UV absorption spectra in Figure 1f show that electronic excitations by the pump wavelength of 243 nm are similar in nature for all ortho-substituted thiophenols.

For 2-FTP-d_1, the channel from the $^1\pi\sigma^*$ state is dominant at 243 nm, although the channel at the low translational energy originating from the $1^1\pi\pi^*$ state (mediated by the $^1\pi\sigma^*$ state) still remains in the range 10−20 kcal/mol, as represented as the gray dashed line in Figure 1b (<10% portion).[12] The total translational energy distribution for 2-CTP-d_1 (Figure 1c) suggests an additional channel at the higher translational energy (olive dashed line) that is higher for 2-BTP-d_1 (Figure 1d). The portion of this additional channel increases nonmonotonically with an increase in the power of the laser pulse, indicating that the multiphoton process should be involved. The $\tilde{X}/\tilde{A}$ branching ratios obtained from the fits considering these factors to the experiment are summarized in Table 1 together with the weighted average values of β for all of the thiophenols studied in this work. The values for thiophenol-d_1 ($\tilde{X}/\tilde{A}$ = 0.78, β = −0.73) agree with previously reported data.[15,18] Notably, the $\tilde{X}/\tilde{A}$ ratios for all of the ortho-substituted thiophenols (0.53−0.66) are significantly lower than that of thiophenol-d_1.

When the reactive flux is directly excited to the repulsive state, the topography of the torsional surface at the Franck−Condon region strongly dictates the nonadiabatic dynamics, although the product branching ratio is determined at CI-2 placed near the asymptotic limit (Figure 2). Even for the initial

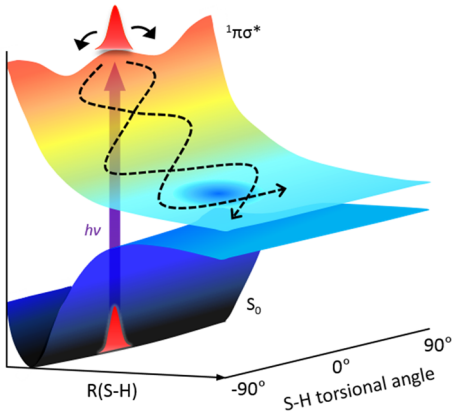

Figure 2. Schematic of the potential energy surfaces and reaction pathways. Initial excitation of the repulsive surface with the S−H torsional angle $\phi \neq 0$ at the Franck−Condon region induces the spread of the reactive flux, thus leading to the dominant $\tilde{A}$ state radical channel. Oscillatory drawing of the wavepacket along the CCS-H(D) dihedral angle in this cartoon is arbitrary, and it is just for showing the conceptual explanation for how to avoid nonadiabatic transition by the out-of-plane nuclear motions at the conical intersection.

optical transition to the bound $2^1\pi\pi^*$ state the S−D bond dissociation, presumably following the ultrafast S_3-S_2 internal conversion, seems to take place promptly on the lower-lying $^1\pi\sigma^*$ state as the near limiting values of β imply. We calculated the torsional PECs of the four lowest singlet states of S_0, S_1, S_2, and S_3 along ϕ for all of the thiophenols studied here using the EOM-CCSD method in order to explain the experimental results, Figure 3. As reported previously, the torsional PECs of thiophenol for the excited states including the $^1\pi\sigma^*$ state display minima at the planar geometries (ϕ = 0°).[21] On the contrary, as shown in Figure 3, the excited-state PECs for the ortho-substituted thiophenols in the Franck−Condon region exhibit lower energies for the nonplanar structures in the range ϕ = 20−45° than at ϕ = 0°. For the $^1\pi\sigma^*$ (S_2) state, for instance, this energy difference is predicted to be highest (180 cm^{-1}) for 2-FTP and lowest (6 cm^{-1}) for 2-CTP. Thus, from a

DOI: 10.1021/acs.jpca.9b00803
J. Phys. Chem. A XXXX, XXX, XXX−XXX

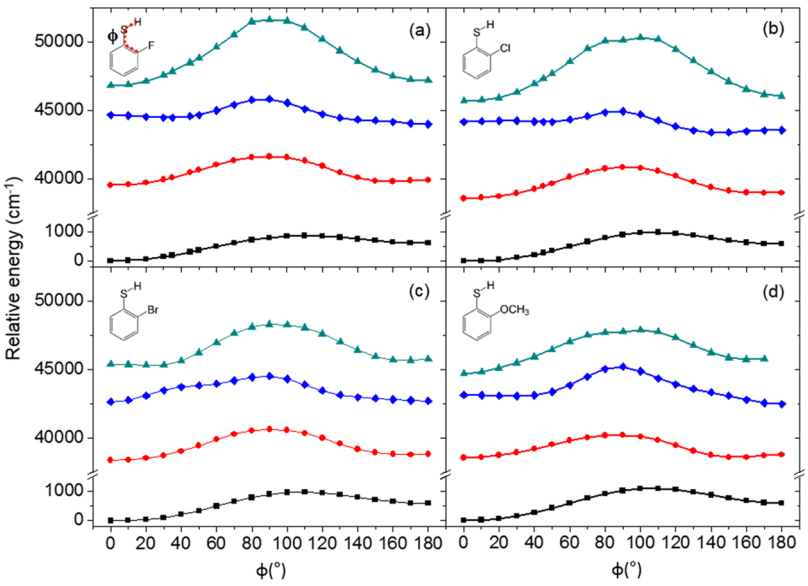

Figure 3. Torsion potential energy curves (PECs) along the CCS−H(D) torsional angle ϕ for the S_0 (black square), S_1 (red dot), S_2 (blue diamond), and S_3 (dark cyan triangle) states of (a) 2-FTP, (b) 2-CTP, (c) 2-BTP, and (d) 2-MTP. S_0 energies and vertical excitation energies were calculated at the CCSD and EOM-CCSD/aug-cc-pVTZ levels of theory, respectively.

simple two-dimensional concept as depicted in Figure 2, 2-FTP is expected to exhibit the largest spread of the initial wavepacket along ϕ at the starting point on the way down to the repulsive state owing to the torsional torque given to the reactive flux sliding on the nonplanar S_2. This will make the flux to avoid the CI-2 quite effectively to afford the lowest $\tilde{X}/\tilde{A}$ ratio among the ortho-substituted thiophenols, which is consistent with the estimated ratio in Table 1. The PEC of 2-CTP for the $^1\pi\sigma^*$ state, on the other hand, is quite shallow, giving the highest $\tilde{X}/\tilde{A}$ ratio among the ortho-substituted thiophenols, which is again consistent with the experimental results. The PEC for the $^1\pi\sigma^*$ state of 2-BTP does not display this feature; however, for the $2^1\pi\pi^*$ (S_3) state this molecule exhibits a nonplanar minimum at 20°. Excitation to the $2^1\pi\pi^*$ state can then induce torsional activity of the reactive flux undergoing the S_2−S_3 internal conversion, leading to the spread with respect to ϕ on the repulsive S_2 surface along which the flux ends up with the less favorable nonadiabatic bifurcation at the CI-2. It is interesting to note that the torsional PECs calculated using TD-DFT (Figure S1) remarkably resemble the high-level EOM-CCSD PECs.

4. CONCLUSIONS

In this study, the effects of ortho substitution on the nonadiabatic reaction dynamics occurring on the excited states have been investigated by VMI combined with high-level ab initio calculations. It is revealed that at 243 nm the nonadiabatic transition probability decreases substantially for all of the ortho-substituted thiophenols studied here relative to that of bare thiophenol. The simple two-dimensional model based on the high-level ab initio potential energy surfaces calculated along the CCS−H(D) out-of-plane torsional coordinate in the Franck−Condon region could explain the experiment quite well, namely, contrary to the planar minima for the excited states of thiophenol, the minima for the 2-FTP, 2-CTP, 2-BTP, and 2-MTP molecules occur at the nonplanar structures. The reactive flux that is excited to the repulsive surface with the initial center in the planar geometry immediately experiences torque along the torsional coordinate as the S−D bond elongation proceeds. Therefore, this initial spread at the starting point leads to increased torsional activity and prefers the adiabatic pathways at the CI-2, thereby generating more $\tilde{A}$ state radicals for the ortho-substituted thiophenols. This work demonstrates that the topology of the excited potential energy surface along the critical nonadiabatic coupling mode may dictate the adiabaticity of the whole chemical reaction processes.

■ ASSOCIATED CONTENT

Supporting Information

The Supporting Information is available free of charge on the ACS Publications website at DOI: 10.1021/acs.jpca.9b00803.

Calculation results of the radical energy gaps for all of the molecules studied here, relative energies in the ground state for 2-BTP and 2-MTP, vertical excitation energies and transition dipole moments for 2-BTP and 2-MTP, UV absorption spectra, torsional PECs, and details in the fitting procedure (PDF)

■ AUTHOR INFORMATION

Corresponding Author

*E-mail: sangkyukim@kaist.ac.kr.

ORCID

Sang Kyu Kim: 0000-0003-4803-1327

Present Addresses

†H.S.Y.: LG Chem, LG science park, Seoul 07796, Republic of Korea.

‡S.H.: Samsung Electronics, Yongin, Kyungki-do 17113, Republic of Korea.

Notes

The authors declare no competing financial interest.

■ ACKNOWLEDGMENTS

This work was supported by the National Research Foundation under Project no. NRF-2018R1A2B3004534.

DOI: 10.1021/acs.jpca.9b00803
J. Phys. Chem. A XXXX, XXX, XXX−XXX

REFERENCES

(1) Sobolewski, A. L.; Domcke, W. Ab initio investigations on the photophysics of indole. *Chem. Phys. Lett.* **1999**, *315*, 293−298.
(2) Sobolewski, A. L.; Domcke, W. Conical intersections induced by repulsive 1$\pi\sigma^*$ states in planar organic molecules: Malonaldehyde, pyrrole and chlorobenzene as photochemical model systems. *Chem. Phys.* **2000**, *259*, 181−191.
(3) Sobolewski, A. L.; Domcke, W. Photoinduced electron and proton transfer in phenol and its clusters with water and ammonia. *J. Phys. Chem. A* **2001**, *105*, 9275−9283.
(4) Sobolewski, A. L.; Domcke, W.; Dedonder-Lardeux, C.; Jouvet, C. Excited-state hydrogen detachment and hydrogen transfer driven by repulsive 1 $\pi\sigma^*$ states: A new paradigm for nonradiative decay in aromatic biomolecules. *Phys. Chem. Chem. Phys.* **2002**, *4*, 1093−1100.
(5) Ashfold, M. N. R.; Devine, A. L.; Dixon, R. N.; King, G. A.; Nix, M. G. D.; Oliver, T. A. A. Exploring nuclear motion through conical intersections in the UV photodissociation of phenols and thiophenol. *Proc. Natl. Acad. Sci. U. S. A.* **2008**, *105*, 12701−12706.
(6) Dixon, R. N.; Oliver, T. A. A.; Ashfold, M. N. R. Tunnelling under a conical intersection: Application to the product vibrational state distributions in the UV photodissociation of phenols. *J. Chem. Phys.* **2011**, *134*, 194303.
(7) Yang, K. R.; Xu, X.; Zheng, J.; Truhlar, D. G. Full-dimensional potentials and state couplings and multidimensional tunneling calculations for the photodissociation of phenol. *Chem. Sci.* **2014**, *5*, 4661−4680.
(8) Lim, J. S.; Kim, S. K. Experimental probing of conical intersection dynamics in the photodissociation of thioanisole. *Nat. Chem.* **2010**, *2*, 627.
(9) Roberts, G. M.; Hadden, D. J.; Bergendahl, L. T.; Wenge, A. M.; Harris, S. J.; Karsili, T. N. V.; Ashfold, M. N. R.; Paterson, M. J.; Stavros, V. G. Exploring quantum phenomena and vibrational control in σ^* mediated photochemistry. *Chem. Sci.* **2013**, *4*, 993−1001.
(10) Han, S.; Lim, J. S.; Yoon, J.-H.; Lee, J.; Kim, S.-Y.; Kim, S. K. Conical intersection seam and bound resonances embedded in continuum observed in the photodissociation of thioanisole-d3. *J. Chem. Phys.* **2014**, *140*, 054307.
(11) Kim, S.-Y.; Lee, J.; Kim, S. K. Conformer specific nonadiabatic reaction dynamics in the photodissociation of partially deuterated thioanisoles (C6H5S-CH2D and C6H5S-CHD2). *Phys. Chem. Chem. Phys.* **2017**, *19*, 18902−18912.
(12) Woo, K. C.; Kang, D. H.; Kim, S. K. Real-time observation of nonadiabatic bifurcation dynamics at a conical intersection. *J. Am. Chem. Soc.* **2017**, *139*, 17152−17158.
(13) Li, S. L.; Truhlar, D. G. Full-dimensional ground- and excited-state potential energy surfaces and state couplings for photodissociation of thioanisole. *J. Chem. Phys.* **2017**, *146*, 064301.
(14) Lim, J. S.; You, H. S.; Kim, S.-Y.; Kim, S. K. Experimental observation of nonadiabatic bifurcation dynamics at resonances in the continuum. *Chem. Sci.* **2019**, *10*, 2404−2412.
(15) Lim, J. S.; Lim, I. S.; Lee, K.-S.; Ahn, D.-S.; Lee, Y. S.; Kim, S. K. Intramolecular orbital alignment observed in the photodissociation of [D1]thiophenol. *Angew. Chem., Int. Ed.* **2006**, *45*, 6290−6293.
(16) Eppink, A. T. J. B.; Parker, D. H. Velocity map imaging of ions and electrons using electrostatic lenses: Application in photoelectron and photofragment ion imaging of molecular oxygen. *Rev. Sci. Instrum.* **1997**, *68*, 3477−3484.
(17) Devine, A. L.; Nix, M. G. D.; Dixon, R. N.; Ashfold, M. N. R. Near-ultraviolet photodissociation of thiophenol. *J. Phys. Chem. A* **2008**, *112*, 9563−9574.
(18) Lim, J. S.; Choi, H.; Lim, I. S.; Park, S. B.; Lee, Y. S.; Kim, S. K. Photodissociation dynamics of thiophenol-d1: The nature of excited electronic states along the S−D bond dissociation coordinate. *J. Phys. Chem. A* **2009**, *113*, 10410−10416.
(19) You, H. S.; Han, S.; Lim, J. S.; Kim, S. K. ($\pi\pi^*/\pi\sigma^*$) conical intersection seam experimentally observed in the S−D bond dissociation reaction of thiophenol-d1. *J. Phys. Chem. Lett.* **2015**, *6*, 3202−3208.
(20) Lim, J. S.; Lee, Y. S.; Kim, S. K. Control of intramolecular orbital alignment in the photodissociation of thiophenol: Conformational manipulation by chemical substitution. *Angew. Chem., Int. Ed.* **2008**, *47*, 1853−1856.
(21) Oliver, T. A. A.; King, G. A.; Tew, D. P.; Dixon, R. N.; Ashfold, M. N. R. Controlling electronic product branching at conical intersections in the UV photolysis of para-substituted thiophenols. *J. Phys. Chem. A* **2012**, *116*, 12444−12459.
(22) Han, S.; You, H. S.; Kim, S.-Y.; Kim, S. K. Dynamic role of the intramolecular hydrogen bonding in nonadiabatic chemistry revealed in the UV photodissociation reactions of 2-fluorothiophenol and 2-chlorothiophenol. *J. Phys. Chem. A* **2014**, *118*, 6940−6949.
(23) You, H. S.; Han, S.; Yoon, J.-H.; Lim, J. S.; Lee, J.; Kim, S.-Y.; Ahn, D.-S.; Lim, J. S.; Kim, S. K. Structure and dynamic role of conical intersections in the $\pi\sigma^*$-mediated photodissociation reactions. *Int. Rev. Phys. Chem.* **2015**, *34*, 429−459.
(24) Marchetti, B.; Karsili, T. N. V.; Cipriani, M.; Hansen, C. S.; Ashfold, M. N. R. The near ultraviolet photodissociation dynamics of 2- and 3-substituted thiophenols: Geometric vs. electronic structure effects. *J. Chem. Phys.* **2017**, *147*, 013923.
(25) Ovejas, V.; Fernández-Fernández, M.; Montero, R.; Longarte, A. On the ultrashort lifetime of electronically excited thiophenol. *Chem. Phys. Lett.* **2016**, *661*, 206−209.
(26) Venkatesan, T. S.; Ramesh, S. G.; Lan, Z.; Domcke, W. Theoretical analysis of photoinduced H-atom elimination in thiophenol. *J. Chem. Phys.* **2012**, *136*, 174312.
(27) Choi, H.; Park, Y. C.; Lee, Y. S.; An, H.; Baeck, K. K. Theoretical study of the extremely small torsional barriers of thiophenol in the ground and the first excited electronic states. *Chem. Phys. Lett.* **2013**, *580*, 32−36.
(28) An, H.; Choi, H.; Lee, Y. S.; Baeck, K. K. Factors affecting the branching ratio of photodissociation: Thiophenol studied through quantum wavepacket dynamics. *ChemPhysChem* **2015**, *16*, 1529−1534.
(29) Lin, G.-S.-M.; Xie, C.; Xie, D. Three-dimensional diabatic potential energy surfaces for the photodissociation of thiophenol. *J. Phys. Chem. A* **2017**, *121*, 8432−8439.
(30) Zhang, L.; Truhlar, D. G.; Sun, S. Electronic spectrum and characterization of diabatic potential energy surfaces for thiophenol. *Phys. Chem. Chem. Phys.* **2018**, *20*, 28144−28154.
(31) Devine, A. L.; Nix, M. G. D.; Cronin, B.; Ashfold, M. N. R. Near-UV photolysis of substituted phenols, I: 4-fluoro-, 4-chloro- and 4-bromophenol. *Phys. Chem. Chem. Phys.* **2007**, *9*, 3749−3762.
(32) Sage, A. G.; Oliver, T. A. A.; King, G. A.; Murdock, D.; Harvey, J. N.; Ashfold, M. N. R. UV photolysis of 4-iodo-, 4-bromo-, and 4-chlorophenol: Competition between C−Y (Y = halogen) and O−H bond fission. *J. Chem. Phys.* **2013**, *138*, 164318.
(33) Li, W.; Chambreau, S. D.; Lahankar, S. A.; Suits, A. G. Megapixel ion imaging with standard video. *Rev. Sci. Instrum.* **2005**, *76*, 063106.
(34) Dribinski, V.; Ossadtchi, A.; Mandelshtam, V. A.; Reisler, H. Reconstruction of Abel-transformable images: The Gaussian basis-set expansion Abel transform method. *Rev. Sci. Instrum.* **2002**, *73*, 2634−2642.
(35) Becke, A. D. Density-functional exchange-energy approximation with correct asymptotic behavior. *Phys. Rev. A: At., Mol., Opt. Phys.* **1988**, *38*, 3098−3100.
(36) El Azhary, A.; Rauhut, G.; Pulay, P.; Werner, H.-J. Analytical energy gradients for local second-order Mo/ller−Plesset perturbation theory. *J. Chem. Phys.* **1998**, *108*, 5185−5193.
(37) Cheng, C.-W.; Lee, Y.-P.; Witek, H. A. Theoretical investigation of molecular properties of the first excited state of the thiophenoxyl radical. *J. Phys. Chem. A* **2008**, *112*, 11998−12006.
(38) Celani, P.; Werner, H.-J. Multireference perturbation theory for large restricted and selected active space reference wave functions. *J. Chem. Phys.* **2000**, *112*, 5546−5557.
(39) Korona, T.; Werner, H.-J. Local treatment of electron excitations in the EOM-CCSD method. *J. Chem. Phys.* **2003**, *118*, 3006−3019.

DOI: 10.1021/acs.jpca.9b00803
J. Phys. Chem. A XXXX, XXX, XXX−XXX

(40) Hamprecht, F. A.; Cohen, A. J.; Tozer, D. J.; Handy, N. C. Development and assessment of new exchange-correlation functionals. *J. Chem. Phys.* **1998**, *109*, 6264−6271.
(41) Frisch, M. J.; Trucks, G. W.; Schlegel, H. B.; Scuseria, G. E.; Robb, M. A.; Cheeseman, J. R.; Scalmani, G.; Barone, V.; Mennucci, B.; Petersson, G. A.; et al. *Gaussian 09*, Revision D.1; Gaussian Inc.: Wallingford, CT, 2009.
(42) Werner, H.-J.; Knowles, P. J.; Knizia, G.; Manby, F. R.; Schutz, M.; Celani, P.; Korona, T.; Lindh, R.; Mitrushenkov, A.; Rauhut, G.; et al. *MOLPRO, a package of ab initio programs*, version 2010.1; http://www.molpro.net.

DOI: 10.1021/acs.jpca.9b00803
J. Phys. Chem. A XXXX, XXX, XXX−XXX